Ultimate Precision Bound of Quantum and Subwavelength Imaging

Cosmo Lupo[1] and Stefano Pirandola[1,2]

[1]*York Centre for Quantum Technologies (YCQT), University of York, York YO10 5GH, United Kingdom*
[2]*Computer Science, University of York, York YO10 5GH, United Kingdom*

We determine the ultimate potential of quantum imaging for boosting the resolution of a far-field, diffraction-limited, linear imaging device within the paraxial approximation. First, we show that the problem of estimating the separation between two pointlike sources is equivalent to the estimation of the loss parameters of two lossy bosonic channels, i.e., the transmissivities of two beam splitters. Using this representation, we establish the ultimate precision bound for resolving two pointlike sources in an arbitrary quantum state, with a simple formula for the specific case of two thermal sources. We find that the precision bound scales with the number of collected photons according to the standard quantum limit. Then, we determine the sources whose separation can be estimated optimally, finding that quantum-correlated sources (entangled or discordant) can be superresolved at the sub-Rayleigh scale. Our results apply to a variety of imaging setups, from astronomical observation to microscopy, exploiting quantum detection as well as source engineering.

Introduction.—Quantum imaging aims at harnessing quantum features of light to obtain optical images of high resolution beyond the boundary of classical optics. Its range of potential applications is very broad, from telescopy to microscopy and medical diagnosis, and has motivated substantial research activity [1–10]. Typically, quantum imaging is scrutinized to outperform classical imaging in two ways: first to resolve details below the Rayleigh length (sub-Rayleigh imaging) and second to improve the scaling of the precision with the photon number, by exploiting nonclassical states of light. It is well known that a collective state of N quantum particles has an effective wavelength that is N times smaller than individual particles [11–18]. If N independent photons are measured, one expects that the blurring of the image scales as $1/\sqrt{N}$ (known as standard quantum limit or shot-noise limit), while for N entangled photons, one can sometimes achieve a $1/N$ scaling (known as the Heisenberg limit).

In this Letter, we compute the optimal resolution limit of quantum imaging for estimating the linear or angular separation between two pointlike monochromatic sources, by using a linear diffraction-limited imaging device in the far-field regime and within paraxial approximation [19]. We show that the ultimate precision bound scales with the number of photons according to the standard quantum limit, for an arbitrary state of the sources. We then study the precision achievable for sources which are in thermal, discordant, or entangled states. We determine the optimal entangled states that saturate the bound, and we show that sources of quantum-correlated light yield optimal imaging of sub-Rayleigh features, allowing for higher resolution below the Rayleigh length. Our findings generalize the

seminal Ref. [10], which has led to several experimental advances in quantum imaging [20–23].

To achieve our results, we estimate the ultimate precision bound in terms of the quantum Fisher information. The ultimate error of any unbiased estimator of the separation s between two sources is given by the quantum Cramér-Rao bound [12,13]

$$\Delta s \geq \frac{1}{\sqrt{\text{QFI}_s}}, \qquad (1)$$

where QFI_s is the quantum Fisher information. The latter is a function of s, of the features of the optical imaging system, and of the state of the light emitted by the sources. Here, we show that a linear diffraction-limited imaging system in the paraxial approximation is equivalent to a pair of beam splitters, whose transmissivities are functions of the separation (see Fig. 1). Thus, we reduce the estimate of the separation to the estimate of the transmissivity of a beam splitter [24–30]. In this way, not only we are able to compute the quantum Fisher information for any pair of sources but we also determine the optimal sources that saturate the ultimate precision bound.

The quantum model.—Consider the canonical annihilation and creation operators c_1, $c_1^\dagger$ and c_2, $c_2^\dagger$ describing two monochromatic pointlike sources. The sources are separated by distance s and lay on the object plane orthogonal to the optical axis at position $-s/2$ and $s/2$. The imaging system maps the source operators into the image operators a_1, $a_1^\dagger$ and a_2, $a_2^\dagger$, describing the optical field on the image screen. Without loss of generality, we assume that the optical system has a unit-magnification factor. This implies that the point-spread function has the form $T(x, y) = \sqrt{\eta}\psi(x - y)$, where x and y are, respectively, the coordinates on the image and
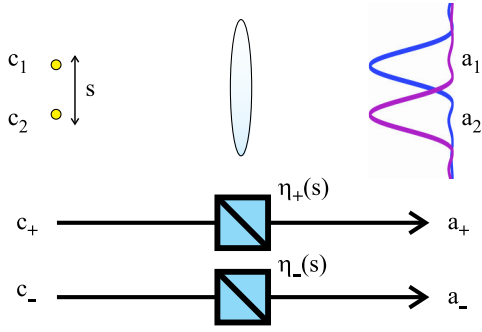
FIG. 1.   A diffraction-limited linear-optical system creating an image of two pointlike sources (top of the figure) is formally equivalent to a pair of independent beam splitters (bottom of the figure), whose transmissivities are functions of the separation between the sources, with $c_\pm = (c_1 \pm c_2)/\sqrt{2}$.

object plane, ψ is a function on the image plane with unit L_2 norm, and η is an attenuation factor. In particular, the image operators read

$$a_1^\dagger = \int dx\, \psi(x+s/2) a_x^\dagger, \quad a_2^\dagger = \int dx\, \psi(x-s/2) a_x^\dagger, \quad (2)$$

where a_x and $a_x^\dagger$ are the canonical creation and annihilation operators for the field at location x on the image screen.

The image modes are distorted and attenuated versions of the source modes. In fact, the optical imaging system transforms the source operators as [31]

$$c_1 \to \sqrt{\eta}\, a_1 + \sqrt{1-\eta}\, v_1, \quad c_2 \to \sqrt{\eta}\, a_2 + \sqrt{1-\eta}\, v_2, \quad (3)$$

where v_1 and v_2 are auxiliary environmental modes that we will assume to be in the vacuum state (this is a physically reasonable assumption at optical frequencies). Because of the nonzero overlap between the two point-spread functions $\psi(x+s/2)$ and $\psi(x-s/2)$, the image operators a_1 and a_2 are not orthogonal; i.e., they do not satisfy the canonical commutation relations. In order to make them orthogonal, we take the sum and difference of the above relations, obtaining

$$c_\pm := \frac{c_1 \pm c_2}{\sqrt{2}} \to \sqrt{\eta_\pm}\, a_\pm + \sqrt{1-\eta_\pm}\, v_\pm, \quad (4)$$

where $\eta_\pm := (1 \pm \delta)\eta$ are transmissivities depending on the image overlap $\delta = \mathrm{Re} \int dx\, \psi^*(x+s/2)\psi(x-s/2)$ between the nonorthogonal modes a_1 and a_2, and

$$a_\pm := \frac{a_1 \pm a_2}{\sqrt{2(1 \pm \delta)}} \quad (5)$$

are orthogonal symmetric and antisymmetric canonical operators on the image plane.

The nonlocal source modes $c_\pm$ are hence independently mapped and attenuated into the image modes $a_\pm$, by means of effective attenuation factors $\eta_\pm = (1 \pm \delta)\eta$, as also shown in Fig. 1. Note that the overlap δ between the two point-spread functions is a crucial parameter in our model: it quantifies the diffraction introduced by the imaging optical

system, as well as the amount of constructive (destructive) interference in the symmetric (antisymmetric) image modes. Also note that this model is well defined only for $\eta \leq 1/2$: we remark that this is in accordance with the fact that in the paraxial approximation a point source is always (by definition) imaged in the far-field regime, in which light is attenuated by a factor $\eta \ll 1$ (see, e.g., Refs. [32,33]) [34].

Our equivalent representation of the imaging process leads to a simple description for the dynamical evolution of the image operators $a_\pm$ in terms of the separation s between the source. In fact, the following lemma holds (see Sec. II of Ref. [35] for the proof).

Lemma 1.—Consider a diffraction-limited linear-optical system creating an image of two pointlike sources. The symmetric and antisymmetric image operators $a_\pm$ satisfy the following dynamical equations in terms of the separation parameter

$$\frac{da_\pm}{ds} = i\omega_\pm [H_\pm^{\mathrm{eff}}, a_\pm], \quad (6)$$

where $H_\pm^{\mathrm{eff}}$ are suitable beam-splitter-like Hamiltonians and $\omega_\pm$ are suitable angular frequencies. We have

$$\omega_\pm = \sqrt{\left(\frac{d\theta_\pm}{ds}\right)^2 + \frac{\epsilon_\pm^2}{4(1 \pm \delta)}}, \quad (7)$$

where $\theta_\pm = \arccos\sqrt{\eta_\pm}$ and

$$\epsilon_\pm^2 = \Delta k^2 \mp \beta - \frac{\gamma^2}{1 \pm \delta}, \quad (8)$$

$$\Delta k^2 := \int dx \left|\frac{d\psi(x)}{dx}\right|^2, \quad \gamma := \frac{d\delta}{ds}, \quad (9)$$

$$\beta := \int dx\, \frac{d\psi(x+s/2)}{dx}\frac{d\psi(x-s/2)}{dx}. \quad (10)$$

Note that the parameters $\epsilon_\pm^2$ in Eq. (8) contain three terms: (i) γ^2 accounts for the variations of the overlap δ due to changes of the separation s, (ii) Δk^2 equals the variance of the momentum operator $-i(d/dx)$ and hence describes translations on the image screen, and (iii) β accounts for interference between the derivatives of the point-spread functions.

Upper bound on the quantum Fisher information.—With Lemma 1, we have shown that estimating the separation between the sources is equivalent to estimating the angle of rotation of a beam-splitter-like transformation. We now obtain the fundamental limits of quantum and sub-Rayleigh imaging by exploiting the fact that the quantum Fisher information for the angle of a beam splitter rotation, when the other input port of the beam splitter is in the vacuum state, is no larger than $4\bar{n}$, where $\bar{n}$ is the mean photon number (see p. 4 of Ref. [24]). In our setting, the fact that the other beam splitter port is in the vacuum state corresponds to the assumption that the only light entering the optical system is that coming from the sources to be imaged; i.e., we are neglecting any source of background radiation, which is a natural assumption at optical frequencies.

Theorem 2.—Consider two pointlike sources with unknown separation s, and emitting a total of $2N$ mean photons, which are observed by an optical system with point-spread function $T(x, y) = \sqrt{\eta}\psi(x - y)$ and attenuation η. Then, the quantum Fisher information cannot exceed the upper bound

$$\mathrm{QFI}_s \leq \frac{2\eta N}{x_R^2} \max\{f_+, f_-\}, \qquad (11)$$

where x_R is the Rayleigh length and the f functions are given by $f_\pm := x_R^2\{\epsilon_\pm^2 + \gamma^2(1 \pm \delta)^{-1}[1 - (1 \pm \delta)\eta]^{-1}\}$.

Proof.—To obtain the upper bound, assume that we can measure not only the image modes $a_\pm$ but also the vacuum modes $v_\pm$ and $b_\pm$. Let us denote as $|\psi'\rangle$ the state of the light of the image modes $a_\pm$ together with the auxiliary modes $v_\pm$ and $b_\pm$.

According to Lemma 1, the dynamics with respect to s is described by the effective beam splitter Hamiltonian $H^{\mathrm{eff}} = \omega_+ H_+^{\mathrm{eff}} + \omega_- H_-^{\mathrm{eff}}$. The upper bound on the quantum Fisher information is therefore obtained by the formula [12,13] $\mathrm{QFI}_s \leq 4\langle\psi'|\Delta^2 H^{\mathrm{eff}}|\psi'\rangle$. The calculation of the right-hand side of this inequality is in Sec. III of Ref. [35], where we use the upper bound of Ref. [24]. In particular, if source $c_\pm$ emits $N_\pm$ mean photons, then we obtain

$$\mathrm{QFI}_s \leq \frac{\eta}{x_R^2}(N_+ f_+ + N_- f_-). \qquad (12)$$

Now, if we fix the total number of photons $2N = N_+ + N_-$, then the maximum is obtained by either $(N_+, N_-) = (2N, 0)$ or $(N_+, N_-) = (0, 2N)$, yielding the bound of Eq. (11). ∎

The upper bound in Eq. (11) is proportional to the mean number of photons $2\eta N$, according to the standard quantum limit. This property is directly inherited from the optimal estimation of a lossy bosonic channel. As expected, the upper bound is inversely proportional to the square of the Rayleigh length x_R, in accordance to the fact that a smaller Rayleigh length allows for higher resolution. Also note that the bound depends on the two functions $f_\pm$, which are the contributions of the nonlocal modes c_+ and c_- to the quantum Fisher information. In general, we expect that for $s \ll x_R$, the symmetric mode is almost insensitive to small variations of s, implying $f_- > f_+ \simeq 0$. On the other hand, for $s \gg x_R$, the two sources decouple, yielding $f_+ \simeq f_-$. Although these functions are smooth, the maximum may occur in correspondence of a crossover, which yields a cusp in the plot of the upper bound; see Fig. 2 and see also Fig. 1 of Ref. [35], where $f_\pm$ are plotted individually. A special case is $\eta = 0.5$, which implies $\eta_+ \simeq 1$ for small s: the symmetric mode is hence perfectly transmitted, yielding $f_+ > f_-$ almost everywhere.

Achievability: Optimal states.—Now, we show that the upper bound established in Theorem 2 can in fact be achieved. Before presenting optimal states saturating the bound, we derive the quantum Fisher information for the
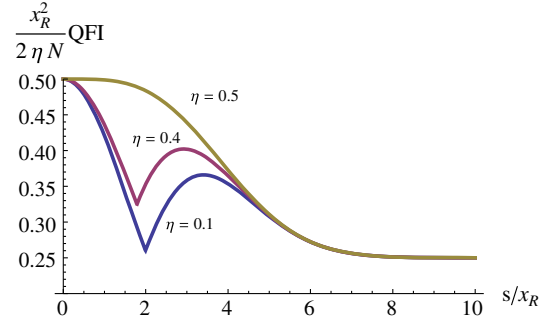

FIG. 2. Ultimate precision bound for the estimation of the separation between two pointlike sources, measured in Rayleigh units. The plot shows the ultimate quantum Fisher information per photon, for a Gaussian point-spread function. From bottom to top, we consider the following optical attenuation $\eta = 0.1, 0.4$, and 0.5. The corresponding functions $f_\pm$ are plotted in Fig. 1 of Ref. [35].

case where the state of the light impinging on the image screen takes the form

$$\rho_{a_+ a_-} = \sum_{n,m} p_{nm}|n, m\rangle\langle n, m|, \qquad (13)$$

where $|n, m\rangle$ is a Fock state with n photons in the symmetric mode and m photons in the antisymmetric one.

The quantum Fisher information for the parameter s can be computed from $\mathrm{QFI}_s = \mathrm{Tr}(\mathcal{L}_s^2 \rho)$, where $\mathcal{L}_s$ is the symmetric logarithmic derivative. For states as in Eq. (13) and given that the modes $c_\pm$ emit $N_\pm$ mean photons each, we obtain

$$\mathrm{QFI}_s = \langle(\partial_s \log p)^2\rangle + \eta N_+ \epsilon_+^2 + \eta N_- \epsilon_-^2, \qquad (14)$$

where $\langle(\partial_s \log p)^2\rangle = \sum_{nm} p_{nm}(\partial_s \log p_{nm})^2$. See Sec. IV of Ref. [35] for proof. Sources as in Eq. (13) include thermal states and two-mode squeezed states, whose quantum Fisher information is computed in Sec. V of Ref. [35].

The case of thermal states is particularly important since most natural sources of light are thermal, especially in astronomical observations. For two sources emitting N thermal photons each, we obtain

$$\mathrm{QFI}_s^{\mathrm{thermal}} = 2\eta N\left[\Delta k^2 - \frac{\eta N(1 + \eta N)\gamma^2}{(1 + \eta N)^2 - \delta^2 \eta^2 N^2}\right]. \qquad (15)$$

This result extends that of Ref. [10] for highly attenuated incoherent sources to the case of thermal sources of any intensity. A comparison with Eq. (11) shows that thermal light is always suboptimal for estimating the separation between the sources, apart from the region $s \gg x_R$, where we obtain $\mathrm{QFI}_s^{\mathrm{thermal}} \simeq \eta N \Delta k^2$. An interesting regime is that of highly attenuated light ($\eta N \ll 1$), in which case we find $\mathrm{QFI}_s^{\mathrm{thermal}} \simeq \eta N \Delta k^2$ for all values of the separation s.

From Eq. (14), it follows that the optimal states among number-diagonal states are those maximizing $\langle(\partial_s \log p)^2\rangle$, which incidentally is the classical Fisher information of

the probability distribution p_{nm} [41]. This observation is exploited for proving the following result.

Theorem 3.—For integer $2N$, the upper bound of Theorem 2 is saturated by sources c_+ and c_- emitting the Fock state $|N_+, N_-\rangle$ with $N_+ + N_- = 2N$. In particular, the optimal state is either $|+\rangle := |2N, 0\rangle$ or $|-\rangle := |0, 2N\rangle$. In terms of the original source modes c_1 and c_2, these are the entangled states

$$|\pm\rangle = \frac{1}{2^N} \sum_{j=0}^{2N} \sqrt{\binom{2N}{j}} (\pm 1)^{2N-j} |j\rangle_1 |2N - j\rangle_2, \quad (16)$$

where $|k\rangle_{1,2}$ is a Fock state for $c_{1,2}$.

Proof.—Since each mode $c_\pm$ is independently attenuated by a attenuation factor $\eta_\pm$, the source state $|N_+, N_-\rangle = (N_+! N_-!)^{-1/2} (c_+^\dagger)^{N_+} (c_-^\dagger)^{N_-} |0\rangle$ is mapped into an image state of the form (13) with $p_{nm} = p_n^+ p_m^-$ and $p_n^\pm = \binom{N_\pm}{n} \eta_\pm^n (1 - \eta_\pm)^{N_\pm - n}$. For such a state, we obtain

$$\langle (\partial_s \log p)^2 \rangle = \frac{\eta N_+ \gamma^2}{(1+\delta)[1-(1+\delta)\eta]} + \frac{\eta N_- \gamma^2}{(1-\delta)[1-(1-\delta)\eta]}.$$

Inserting this result into Eq. (14), we obtain that the Fock state $|N_+, N_-\rangle$ yields $\mathrm{QFI}_s = \eta / x_R^2 (N_+ f_+ + N_- f_-)$. The maximum of this quantity under the constraint $N_+ + N_- = 2N$ is obtained by putting either $N_+ = 2N$ or $N_+ = 0$, hence saturating the upper bound of Theorem 2. ∎

We remark that the optimal states in Theorem 3 have the same form of the optimal states for the estimation of the loss parameter of a bosonic channel [25]. Following Ref. [25], optimal states for noninteger $2N$ can be approximated by superposition of Fock states with different photon numbers. Sources emitting photons in a two-mode squeezed vacuum and sources of separable but quantum-correlated thermal light exhibit features similar to the optimal states (see Secs. V. B and V. C of Ref. [35]).

Ultimate quantum Fisher information.—Having found a matching lower bound implies that Eq. (11) is in fact achievable and represents the ultimate quantum Fisher information, optimized over the state of the light emitted by the sources. It is clear that optimal states can be explicitly engineered in all those scenarios where we can control the light emitted by the sources, which is a typical case in microscopy.

For $s \gg x_R$, the overlap δ between the image modes becomes negligible; hence, Eq. (11) yields $\mathrm{QFI}_s \simeq 2\eta N \Delta k^2 \sim 2\eta N x_R^{-2}$. On the other hand, for generic values of the separation s and all values of the optical attenuation η, we find $\mathrm{QFI}_s > 2\eta N \Delta k^2$. This means that the closer the sources are, the better their distance can be estimated. This counterintuitive phenomenon is a superresolution effect which appears at the sub-Rayleigh scale for entangled sources. We have also found examples of quantum-correlated sources that are not entangled (but discordant)

which displays superresolution at the sub-Rayleigh scale (see Sec. V. C of Ref. [35]).

The superresolution is explicitly shown in the example of Fig. 2, where we consider a Gaussian point-spread function $\psi(x) \sim \exp[-x^2/(4x_R^2)]$ with variance x_R^2. In this case, $\Delta k^2 = 1/(4x_R^2)$, which yields $\lim_{s \gg x_R} \mathrm{QFI}_s = 2\eta N \Delta k^2 = \eta N / (2 x_R^2)$. Figure 2 shows the ultimate (normalized) quantum Fisher information per photon, i.e., $x_R^2 \mathrm{QFI}_s / (2\eta N)$, versus the dimensionless separation s/x_R. The maximum value of the quantum Fisher information per photon is $1/2$, which is reached for $s/x_R \to 0$.

Optimal measurements at the sub-Rayleigh scale.—We now present a suboptimal measurement that is optimal for $s \lesssim x_R$. We consider sources emitting light in the optimal state as in Theorem 3. We also consider a standard setting where the point-spread function is symmetric around its center, i.e., $\psi(x - y) = \psi(|x - y|)$. It follows that the image modes

$$a_\pm^\dagger = \frac{1}{\sqrt{2(1 \pm \delta)}} \int dx [\psi(x + s/2) \pm \psi(x - s/2)] a_x^\dagger \quad (17)$$

are, respectively, even and odd functions of the coordinate x. We can hence consider a measurement able to distinguish the parity as, for example, photodetection of the Hermite-Gauss modes. (This kind of measurement is optimal also in other settings [10]. See also Ref. [42] for a more general approach.)

Consider photon counting in the space of even and odd functions. The probability of counting n photons in even modes is given by p_n^+, and the probability of n photons in odd modes is given by p_n^-. The (classical) Fisher information associated with this measurement is

$$F_s = \frac{\eta N_+ \gamma^2}{(1+\delta)(1-(1+\delta)\eta)} + \frac{\eta N_- \gamma^2}{(1-\delta)(1-(1-\delta)\eta)}. \quad (18)$$

For $s \lesssim x_R$, this nonadaptive measurement is optimal for almost all values of η (but for $\eta \sim 0.5$). For larger values of s, it fails to be optimal because it does not account for the fact that a change in the value of the separation s also implies a translation of the image modes on the image screen.

Conclusions.—We have found the ultimate precision bound for estimating the separation between two pointlike sources using a linear-optical imaging system, considering arbitrary quantum states for the sources. Although we have focused on the problem of estimating the separation between two sources, our approach can be immediately extended to the problem of estimating the location of a single source.

Our findings show that the separation between sources emitting quantum-correlated light (entangled or discordant) can be superresolved at the sub-Rayleigh region. In particular, we have found the optimal entangled states with this feature. Under optimal conditions, one can increase the sub-Rayleigh quantum Fisher information by a constant factor with respect of its value for separations much larger than the Rayleigh length. In the sub-Rayleigh regime, we

have shown that photon counting in the symmetric and antisymmetric modes is an optimal measurement.

Another consequence of our findings is that the ultimate accuracy for any linear-optical, far-field imaging system in the paraxial approximation scales according to the standard quantum limit. While, in principle, it could still be possible to beat the standard quantum limit, our results show that in order to do so, it is necessary to rely on a biased estimator for the source separation, to consider nonpointlike sources, or to employ a near-field, nonlinear, or nonparaxial imaging system.

Note added.—The formula for thermal sources [see Eq. (15)] has been independently found by Nair and Tsang [43]; these authors also study tailored measurements that are almost optimal for estimating the separation between two thermal sources.

[1] C. W. Helstrom, *Quantum Detection and Estimation Theory* (Academic, New York, 1976).

[2] M. I. Kolobov and C. Fabre, Phys. Rev. Lett. **85**, 3789 (2000).

[3] V. Giovannetti, S. Lloyd, L. Maccone, and J. H. Shapiro, Phys. Rev. A **79**, 013827 (2009).

[4] M. Tsang, Phys. Rev. Lett. **102**, 253601 (2009).

[5] H. Shin, K. W. C. Chan, H. J. Chang, and R. W. Boyd, Phys. Rev. Lett. **107**, 083603 (2011).

[6] O. Schwartz and D. Oron, Phys. Rev. A **85**, 033812 (2012).

[7] J.-M. Cui, F.-W. Sun, X.-D. Chen, Z.-J. Gong, and G.-C. Guo, Phys. Rev. Lett. **110**, 153901 (2013).

[8] O. Schwartz, J. M. Levitt, R. Tenne, S. Itzhakov, Z. Deutsch, and D. Oron, Nano Lett. **13**, 5832 (2013).

[9] D. Gatto Monticone, K. Katamadze, P. Traina, E. Moreva, J. Forneris, I. Ruo-Berchera, P. Olivero, I. P. Degiovanni, G. Brida, and M. Genovese, Phys. Rev. Lett. **113**, 143602 (2014).

[10] M. Tsang, R. Nair, and X. M. Lu, Phys. Rev. X **6**, 031033 (2016).

[11] S. L. Braunstein, Phys. Rev. Lett. **69**, 3598 (1992).

[12] S. L. Braunstein and C. M. Caves, Phys. Rev. Lett. **72**, 3439 (1994).

[13] S. L. Braunstein, C. M. Caves, and G. J. Milburn, Ann. Phys. (N.Y.) **247**, 135 (1996).

[14] A. N. Boto, P. Kok, D. S. Abrams, S. L. Braunstein, C. P. Williams, and J. P. Dowling, Phys. Rev. Lett. **85**, 2733 (2000).

[15] V. Giovannetti, S. Lloyd, and L. Maccone, Science **306**, 1330 (2004).

[16] M. G. A. Paris, Int. J. Quantum. Inform. **07**, 125 (2009).

[17] U. Dorner, R. Demkowicz-Dobrzanski, B. J. Smith, J. S. Lundeen, W. Wasilewski, K. Banaszek, and I. A. Walmsley, Phys. Rev. Lett. **102**, 040403 (2009).

[18] V. Giovannetti, S. Lloyd, and L. Maccone, Nat. Photonics **5**, 222 (2011).

[19] J. W. Goodman, *Introduction to Fourier Optics* (McGraw-Hill, New York, 1968).

[20] Z. S. Tang, K. Durak, and A. Ling, arXiv:1605.07297.

[21] F. Yang, A. Taschilina, E. S. Moiseev, C. Simon, and A. I. Lvovsky, arXiv:1606.02662.

[22] W.-K. Tham, H. Ferretti, and A. M. Steinberg, arXiv:1606.02666.

[23] M. Paúr, B. Stoklasa, Z. Hradil, L. L. Sánchez-Soto, and J. Rehacek, Optica **3**, 1144 (2016).

[24] A. Monras and M. G. A. Paris, Phys. Rev. Lett. **98**, 160401 (2007).

[25] G. Adesso, F. Dell'Anno, S. De Siena, F. Illuminati, and L. A. M. Souza, Phys. Rev. A **79**, 040305(R) (2009).

[26] O. Pinel, P. Jian, N. Treps, C. Fabre, and D. Braun, Phys. Rev. A **88**, 040102 (2013).

[27] H. Venzl and M. Freyberger, Phys. Rev. A **75**, 042322 (2007).

[28] R. Gaiba and M. G. A. Paris, Phys. Lett. A **373**, 934 (2009).

[29] A. Monras and F. Illuminati, Phys. Rev. A **83**, 012315 (2011).

[30] G. Spedalieri, S. L. Braunstein, and S. Pirandola, arXiv:1602.05958.

[31] To derive this transformation rule, consider a single photon emitted in one of the source modes, say, c_1. The optical system transmits this photon with probability η and transfers it to an environmental mode v_1 with probability $1 - \eta$, i.e., $|\psi\rangle = c_1^\dagger|0\rangle \to (\sqrt{\eta}a_1^\dagger + \sqrt{1-\eta}v_1^\dagger)|0\rangle$.

[32] J. H. Shapiro, IEEE J. Sel. Top. Quantum Electron. **15**, 1547 (2009).

[33] C. Lupo, V. Giovannetti, S. Pirandola, S. Mancini, and S. Lloyd, Phys. Rev. A **85**, 062314 (2012).

[34] The imaging system is characterized by the Fresnel number $\mathcal{F} = \ell/x_R$, where ℓ is the size of the source and x_R is the Rayleigh length. For $\mathcal{F} \ll 1$, the imaging system operates in the far-field regime, in which light is attenuated by a factor $\eta \simeq \mathcal{F}$ [32,33]. By definition, a pointlike source is such that its size is much smaller than the typical size of the imaging system, which in our case is the Rayleigh length. It follows that the optical system operates in the far-field regime and the light is attenuated by a factor $\eta \simeq \mathcal{F} \ll 1$.

[35] See Supplemental Material at http://link.aps.org/supplemental/10.1103/PhysRevLett.117.190802 which includes Refs. [36–40], for proofs of the theorems, details of the calculations and additional plots.

[36] A. Ferraro, S. Olivares, and M. G. A. Paris, *Gaussian States in Quantum Information* (Bibliopolis, Naples, 2005).

[37] C. Weedbrook, S. Pirandola, R. Garcia-Patron, N. J. Cerf, T. C. Ralph, J. H. Shapiro, and S. Lloyd, Rev. Mod. Phys. **84**, 621 (2012).

[38] S. Pirandola, G. Spedalieri, S. L. Braunstein, N. J. Cerf, and S. Lloyd, Phys. Rev. Lett. **113**, 140405 (2014).

[39] G. Adesso and A. Datta, Phys. Rev. Lett. **105**, 030501 (2010).

[40] P. Giorda and M. G. A. Paris, Phys. Rev. Lett. **105**, 020503 (2010).

[41] H. Cramér, *Mathematical Methods of Statistics* (Princeton University Press, Princeton, 1946).

[42] J. Rehacek, M. Paur, B. Stoklasa, L. Motka, Z. Hradil, and L. L. Sanchez-Soto, arXiv:1607.05837.

[43] R. Nair and M. Tsang, preceding Letter, Phys. Rev. Lett. **117**, 190801 (2016).